ESTIMATION LST MAP FOR ORTA CHIRCHIK DISTRICT, UZBEKISTAN USING LANDSAT 8 SATELLITE IMAGES

Farkhod Abdullaev[1], Gantig Unenbuyan[2], Rakhmatulla Ermanov[3], Saidbobir Gaffarov[4]

Abstract — At Remote Sensing field lands surface temperature (LST) described as a digital representation skin temperature of the ground. LST is one of the important factors in Earth Observation studies such as hydrological, environmental, land use land cover change, climate change and agricultural studies. There some methods which are determined by some scientists. Some of these methods are Split-Window Algorithm (SWA) [1, 2, 3, 4, 5], Single Channel Method (SChM) [6, 7, 8] and Radiative Transfer Equation Based Method (RTEBM) [9, 10, 11].

Index Terms — hydrological, environmental, land, climate change and agricultural studies

1 INTRODUCTION

At Remote Sensing field lands surface temperature (LST) described as a digital representation skin temperature of the ground. LST is one of the important factors in Earth Observation studies such as hydrological, environmental, land use land cover change, climate change and agricultural studies. There some methods which are determined by some scientists. Some of these methods are Split-Window Algorithm (SWA) [1, 2, 3, 4, 5], Single Channel Method (SChM) [6, 7, 8] and Radiative Transfer Equation Based Method (RTEBM) [9, 10, 11].

Based on Single Channel Method we developed a model in ArcGIS software Model Maker tool. On any program derivation, LST map takes more time for time series analysis. ArcGIS Model can help take more results reduce process time and do it automatically with the developed model. LST estimation map we can develop Model on any software like ERDAS IMAGINE, ENVI or QGIS. Most researchers use ArcGIS software, so it will be easier for most part of users.

We will determine LST map and Model using Landsat 8 data. The model developed using three bands: B4 (Red-0.64–0.67 micrometres) and B5 (Near Infrared-0.85–0.88 micrometres) for developing NDVI map and B10 (Thermal-10.60–11.19 micrometres) for derivation Land Surface Emissivity (LSE) and LST map.

2 DATA AND METHODS

The model created in ArcGIS software only can use estimation LST by process Landsat 8 30 m spatial resolution data. Because model included Landsat 8 sensor characteristics: rescale factor, reflectance and so on. LST Estimation methodology given below in Figure 1, which we had processed and checked results and developed with the help of Model Maker Tool ArcGIS software.

Landsat 8 satellite image free available on Earth Explorer website (https://earthexplorer.usgs.gov/). In this case develop ArcGIS model we used 2015 Landsat 8 data 154th path, 31st row – Uzbekistan, Tashkent Region. The metadata used of the satellite images in this algorithm is presented in Table 1. Study area given in Fig. 1.

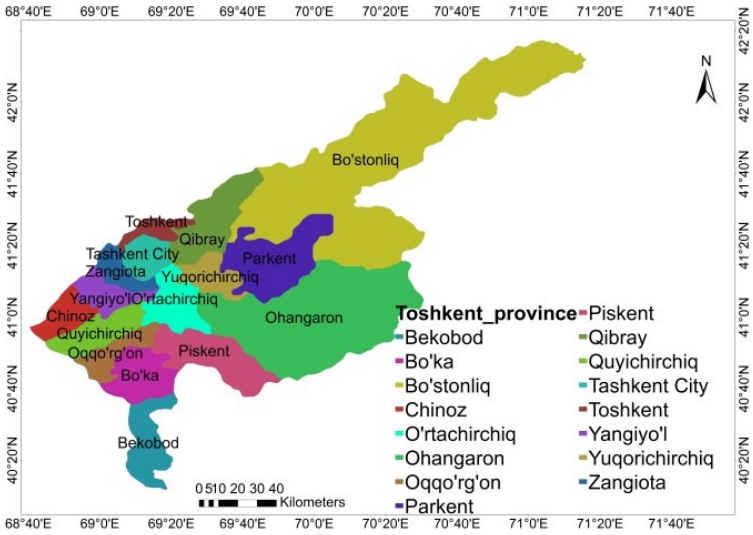

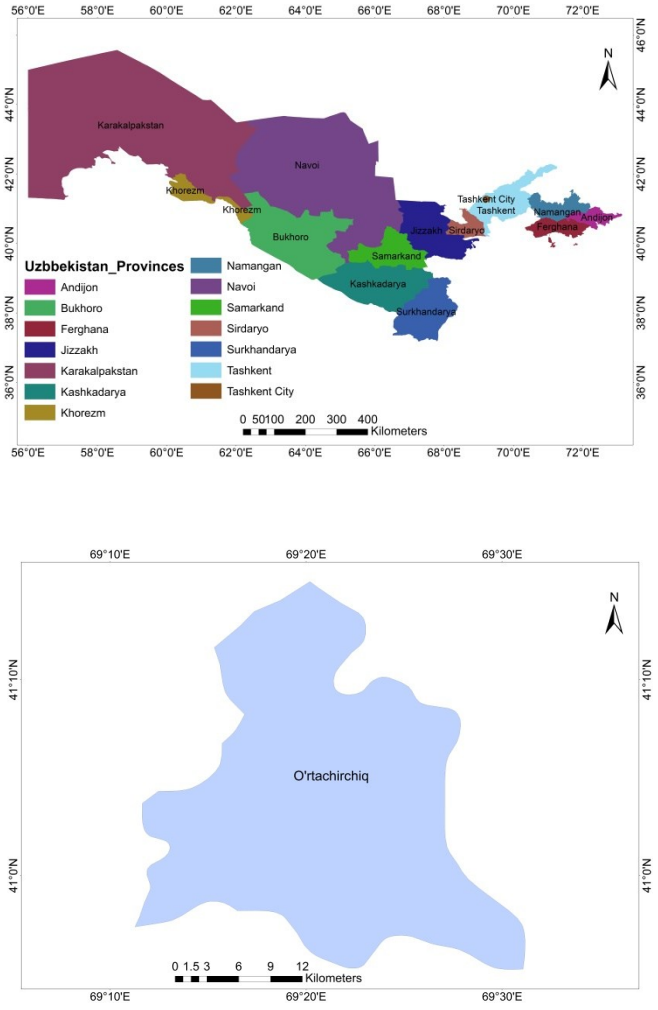

Figure 1. Location of Study area – Orta Chirchik District

2.1. *DN to Radiance.* The first part of the model determines the Band 10. After put input band 10 used formula taken from the USGS web page for retrieving the top of atmospheric (TOA) spectral radiance ($L\lambda$):

$$L\lambda = M_L * Q_{cal} + A_L \quad (1)$$

Where M_L represents the band-specific multiplicative rescaling factor, Q_{cal} is the Band 10 image, A_L is the band-specific additive rescaling factor.

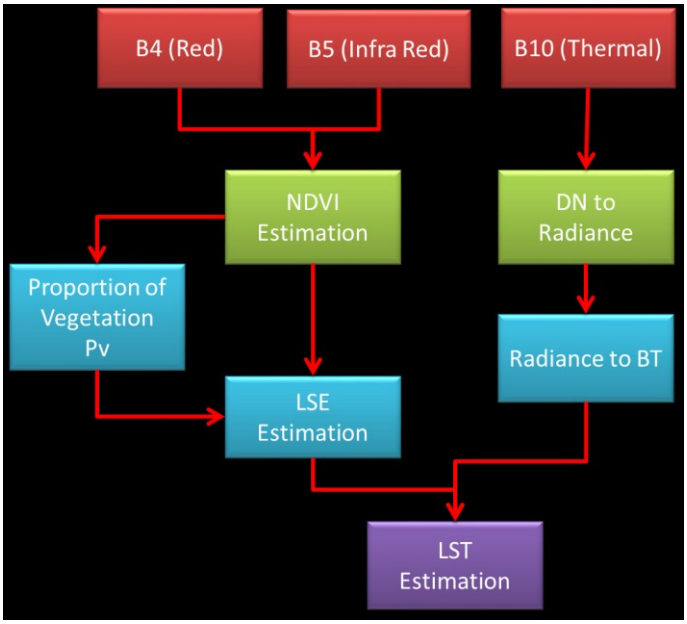

Figure 2. LST Estimation

Table 1. Landsat 8 metadata

Thermal constant, Band 10	
K_1	1321.0789
K_2	774.8853
Rescaling factor, Band 10	
M_L	$3.342x10^{-4}$
A_L	0.1

2.2. *Convert Radiance to Brightness Temperature.* After describing digital numbers (DNs) to radiance, the TIRS band converted from spectral radiance to brightness temperature (BT) using the thermal constants taken from the metadata file. With the following equation given below we used algorithm to convert reflectance to BT [16]:

$$BT = \frac{K_2}{\ln(K_1)} - 273.15 \quad (2)$$

Where K_1 and K_2 stand for the band-specific thermal conversion constants from the metadata.

- *Farkhod Abdullaev[1], Gantig Unenbuyan[2], Rakhmatulla Ermanov[3], Saidbobir Gaffarov[4]*
- *[1]Irrigation Water Saving Technologies Scientific Research Consulting Centre, Uzbekistan;*
- *[2]MONMAP LLC, Mongolia; [3,4]Irrigation and Water Problems Scientific Research Institute, Uzbekistan*

For obtaining the results in Celsius, the radiant temperature is revised by adding the absolute zero (approx. −273.15°C).

2.3. *NDVI based Emissivity Calculation*

2.3.1. *NDVI Calculation.* Landsat 8 satellite image Red and Near Infrared bands we used for calculate the Normal Difference Vegetation Index (NDVI). NDVI is shown vegetation health condition for the satellite passed time over that area. The calculation of the NDVI is important because, after this, the vegetation proportion (Pv) will be calculated, and they are highly related with the NDVI, and Pv should be calculated, which is related to the emissivity (ε):

$$NDVI = \frac{}{} \quad (3)$$

Where NIR represents the Near Infrared band (Band 5) and Red represents the red band (Band 4).

2.3.2. *Calculation of the Vegetation Proportion.* P_V is calculated following to (4). The method for calculating Pv [4] suggests using the NDVI values for [12, 13, 14, 15]:

$$P_V = \left| \frac{}{} \right| \quad (4)$$

Where the $NDVI_S$ is minimum and $NDVI_V$ is maximum NDVI representation values.

2.3.3. *Calculating Land Surface Emissivity.* The land surface emissivity (LSE) must be known in order to estimate LST, since the LSE is a proportionality factor that scales blackbody radiance (Planck's law) to predict emitted radiance, and it is the efficiency of transmitting thermal energy across the surface into the atmosphere. The determination of the ground emissivity is calculated conditionally as suggested in:

$$\varepsilon_\lambda = 0.004 * P_V + 0.986 \quad (5)$$

The last step of retrieving the LST or the emissivity corrected land surface temperature T_S is computed as follows [17]:

$$T_S = \frac{}{} \quad (7)$$

Where T_S is the LST in Celsius (∘C, (2)), BT is at-sensor BT (°C), λ is the wavelength of emitted radiance (for which the peak response and the average of the limiting wavelength (λ=10.895) [15] will be used), ε_λ is the emissivity calculated in (6), and

$$\rho = h - = 1.438 \times 10^{-2}\ m\ K \quad (8)$$

Where σ is the Boltzmann constant (1.38×10^{-23} J/K), h is Planck's constant (6.626×10^{-34} J s), and c is the velocity of light (2.998×10^8 m/s).

4 LIST OF RESULTS AND VALIDATION

4.1. LST Estimation Results. Landsat 8 images for July 30 and September 16 for 2015 downloaded and processed in ArcGIS software. In Model maker Tool developed different products models and finally they are combined into the single flowchart. Therefore, after completed flowchart we run Model given below in Fig. 3.

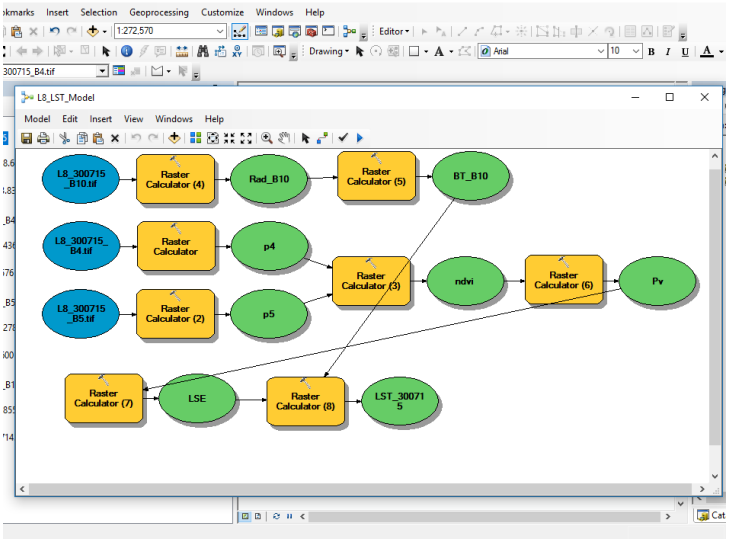

Figure 3. Derived LST Model in ArcGIS

Results LST maps for 30/07 and 16/09 given in Figure 3.LST validation estimated by the MODIS (MYD11A1) data. NASA Land Data Products and Services provide by AQUA and TERRA daily LST Product. Validate Landsat LST map used AQUA 1 km spatial resolution daytime LST Product. First MYD11A1 data downloaded from http://earthexplorer.usgs.gov/, after that converted through MRT MODIS Tool to TIFF from HDF-EOS format. Daytime 1 km LST images clipped for Orta Chirchik District, rescaled and converted from Kelvin to Celsius.

4.2. Comparison of LST Validation Results. To compare LST maps results two different satellite images from same dates in Orta Chirchik District Tashkent Region was chosen.

On 30/07/2015 date derived LST by Landsat 8 map shows 23.8 to 48.6°C, which is highest temperature in Uzbekistan. LST map shows lowest temperature for irrigated areas and water body features, highest temperature for bare lands and built up area features, which is close to Tashkent city. On 16/09/2015 date LST map shows 13.7 to 38.8°C (Figure 5), which is summertime is changing to fall.

MODIS LST map for July 30 shows 30.2 to 48.9°C for different features, including croplands, built-up areas, bare lands and water bodies. LST map for September 16 shows 24.4 to 42.1°C (Figure 6).

Validation Landsat 8 LST map we used MODIS LST map with the scatter plot in MS Excel software. At this scatter plot X-axis used for Landsat 8 LST and for Y-axis MODIS LST. Data validation MODIS and Landsat 8 for July 30 scatter plot match 97.66 % and September 16 match 95.32 % given below in Figure 7.

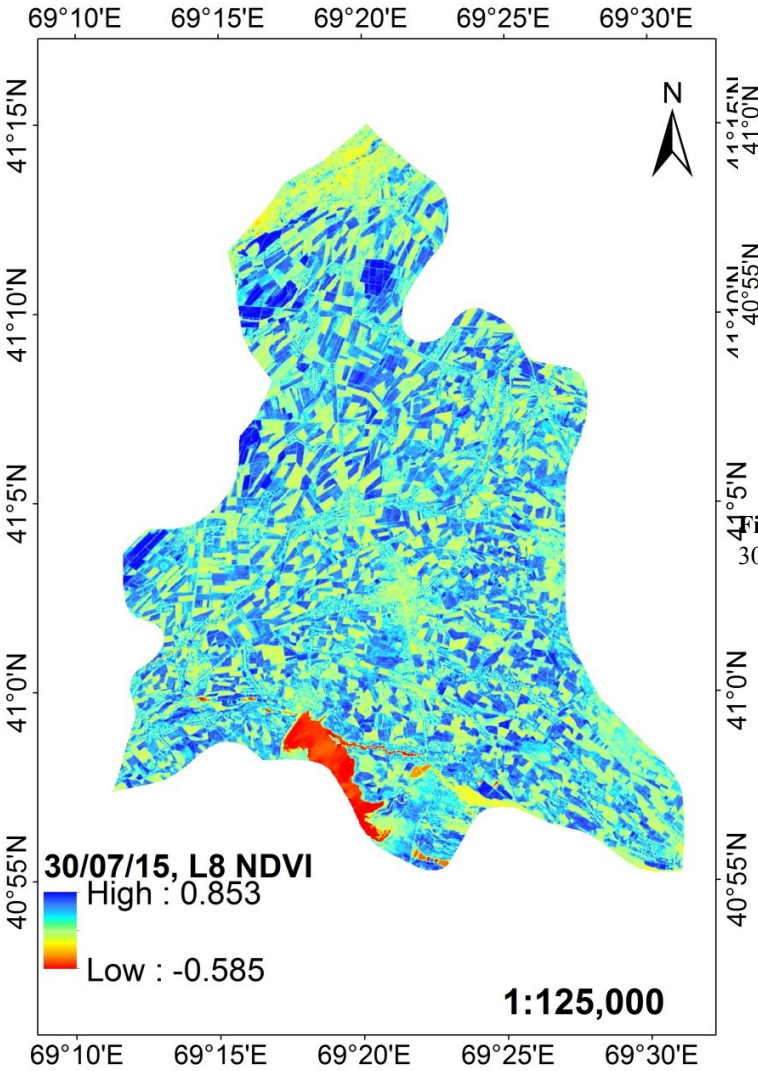

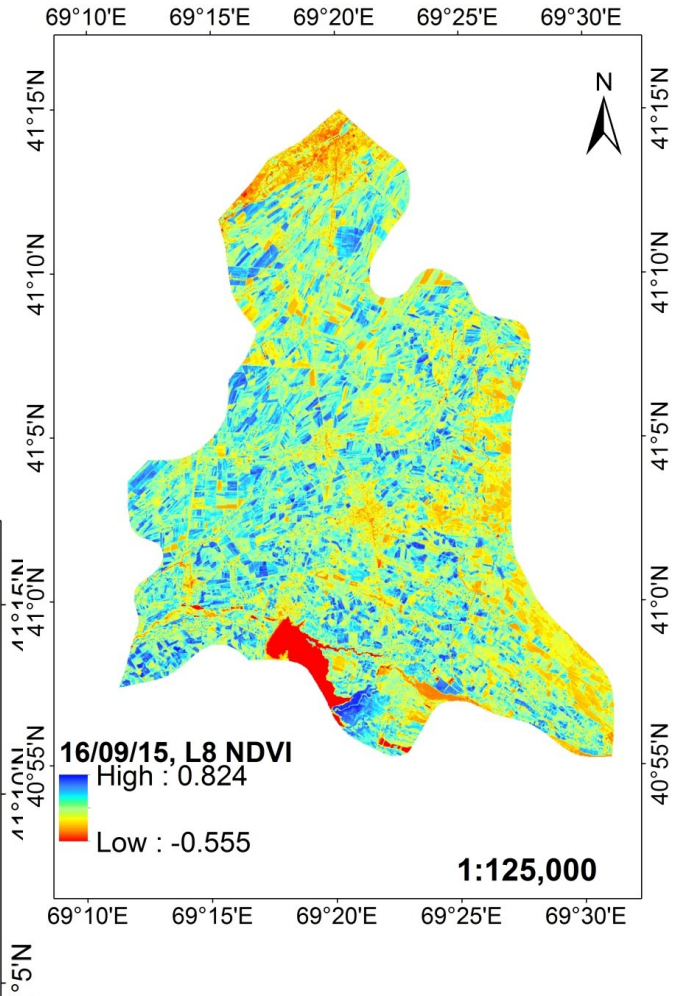

Figure 4. 30 m resolution Landsat 8 derived NDVI maps from July 30 and September 16, 2015

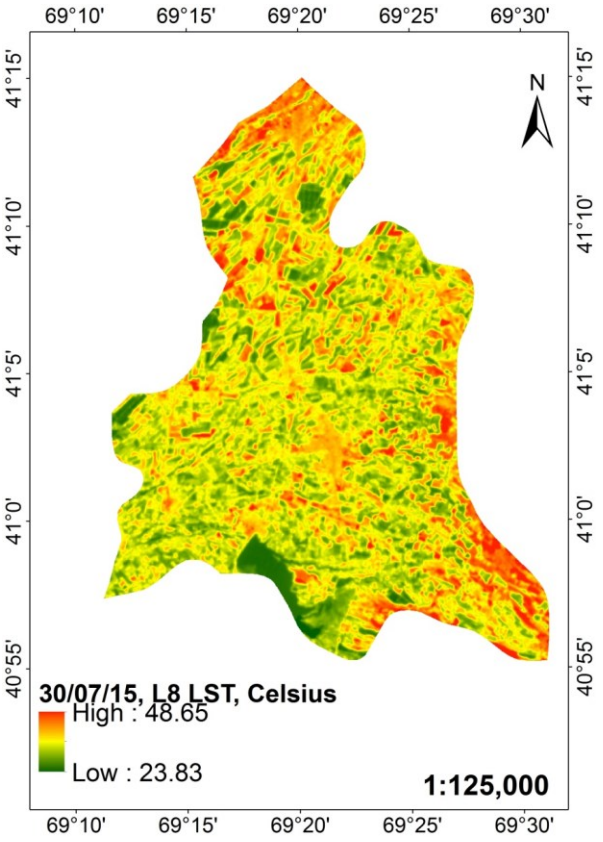

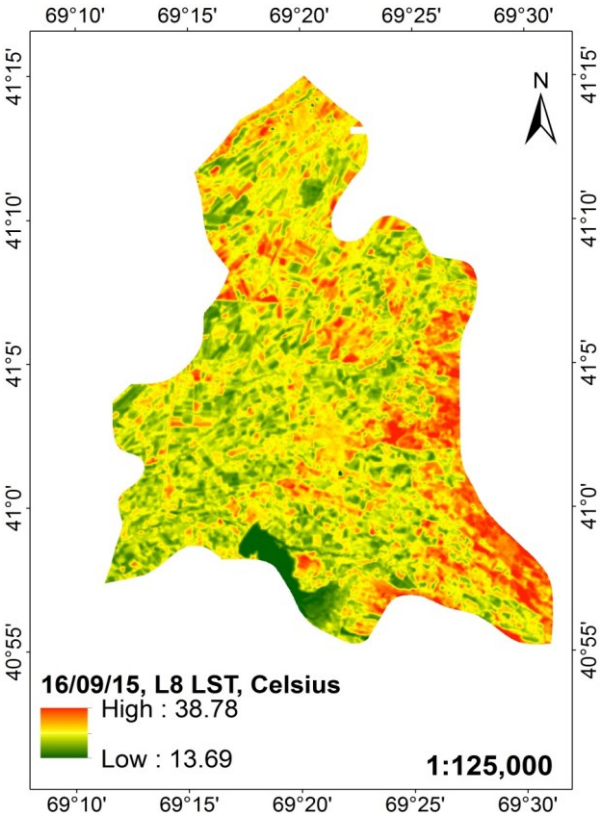

Figure 5. 30 m resolution Landsat 8 derived LST maps from July 30 and September 16, 2015

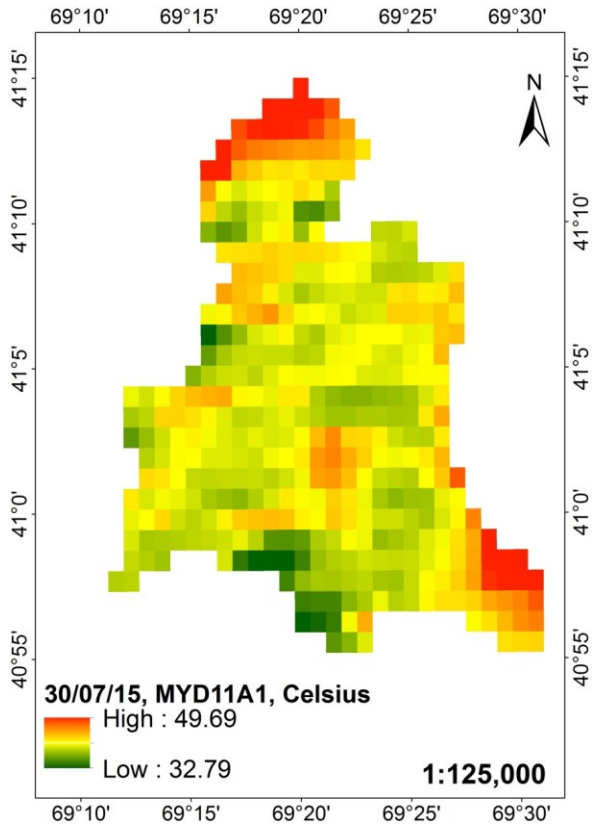

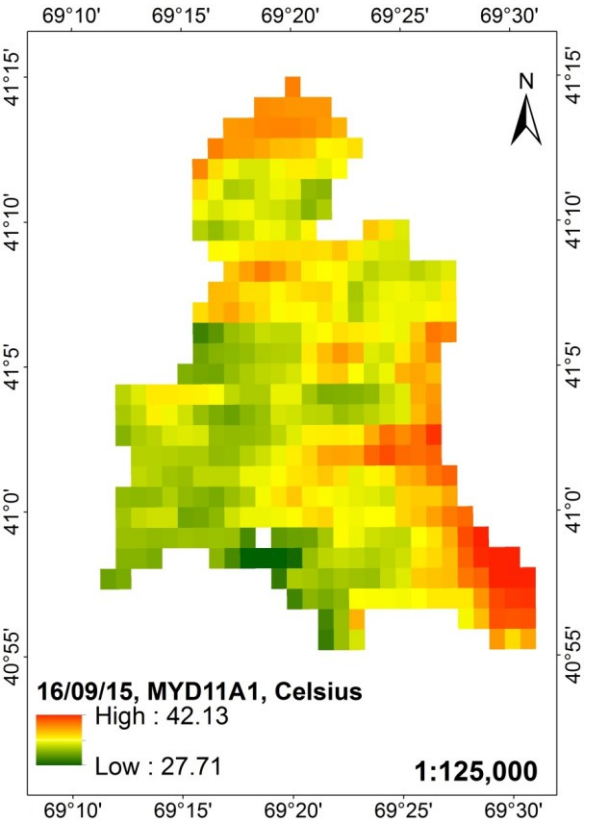

Figure 6. MODIS 1 km resolution LST maps from July 30 and September 16, 2015

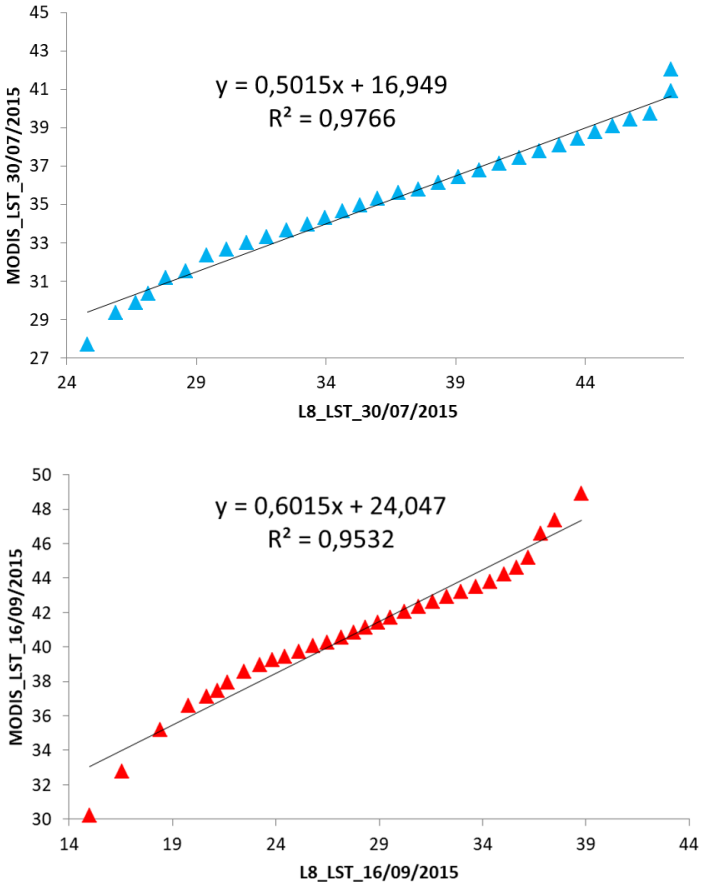

Figure 7. Scatter plot validation of 30 m resolution Landsat 8 LST and MODIS 1 km resolution LST maps from July 30 and September 16, 2015

5 CONCLUSION

The paper presenting complete Model in ArcGIS model maker for derived Landsat 8 LST map use bands Red, Near Infrared and Thermal. Landsat 8 satellite passes for path 153, row 031 every day on 11:06 local time. Final estimated LST maps give low to a high temperature for a land use first water body, irrigated croplands, agriculture fields and last one is built up areas close to the city.

Validation of results has done by MODIS LST map. Because site measurement station we did not consider. In scatter plot by the MS Excel on X (Landsat 8 LST) and Y (MODIS LST) axis. For further studies, the tool can be used for LST Estimation. Validation of results can be determined with the MODIS LST, which is not available situ measurement data.

REFERENCES

[1] F. Becker and Z.-L. Li, "Towards a local split window method over land surfaces," International Journal of Remote Sensing, vol. 11, no. 3, pp. 369–393, 1990.

[2] Wan, Z.; Dozier, J. A generalized split-window algorithm for retrieving land-surface temperature from space. IEEE Trans. Geosci. Remote Sens. 1996, 34, 892–905.

[3] Rozenstein, O.; Qin, Z.; Derimian, Y.; Karnieli, A. Derivation of land surface temperature for Landsat-8 TIRS using a split window algorithm. Sensors 2014, 14, 5768–5780.

[4] Mao K.; Qin, Z.; Shi, J.; Gong, P. The research of split-window algorithm on the MODIS. Geomat. Inf. Sci. Wuhan Univers 2005, 30, 703–707.

[5] Qin, Z.; Dall'Olmo, G.; Karnieli, A.; Berliner, P. Derivation of split window algorithm and its sensitivity analysis for retrieving land surface temperature from NOAA-advanced very high-resolution radiometer data. J. Geophys. Res.: Atmos. 2001, 106, 22655–22670.

[6] Jimenez-Munoz, J.C.; Cristobal, J.; Sobrino, J.A.; Soria, G.; Ninyerola, M.; Pons, X. Revision of the single-channel algorithm for land surface temperature retrieval from Landsat thermal-infrared data. IEEE Trans. Geosci. Remote Sens. 2009, 47, 339–349.

[7] Coll, C.; Caselles, V.; Valor, E.; Niclòs, R. Comparison between different sources of atmospheric profiles for land surface temperature retrieval from single channel thermal infrared data. Remote Sens. Environ. 2012, 117, 199–210.

[8] Jimenez-Munoz, J.C.; Sobrino, J.A. Error sources on the land surface temperature retrieved from thermal infrared single channel remote sensing data. Int. J. Remote Sens. 2006, 27, 999–1014.

[9] Xiaolei, Y., Xulin. G., Zhaocong. W. (2014). Land Surface Temperature Retrieval from Landsat 8 TIRS—Comparison between Radiative Transfer Equation-Based Method, Split Window Algorithm and Single Channel Method, Journal of Remote Sensing, Volume 6 issue 10, 9829-9852.

[10] F. Wang, Z. Qin, C. Song, L. Tu, A. Karnieli, and S. Zhao, "An improved mono-window algorithm for land surface temperature retrieval from Landsat 8 thermal infrared sensor data, "Remote Sensing, vol. 7, no. 4, pp. 4268–4289, 2015.

[11] P. K. Srivastava, T. J. Majumdar, and A. K. Bhattacharya, "Surface temperature estimation in Singhbhum Shear Zone of India using Landsat-7 ETM+ thermal infrared data," Advances in Space Research, vol. 43, no. 10, pp. 1563–1574, 2009.

[12] Tucker, C.J. Red and photographic infrared linear combinations for monitoring vegetation. Remote Sens. Environ., 8, 127–150, 1979

[13] Tarnavsky E., Garrigues S., Brown M.E. Multiscale geostatistical analysis of AVHRR, SPOT-VGT, and MODIS global NDVI products. Remote Sens. Environ., 112, 535–549, 2008

[14] Li P., Jiang L., Feng Z. Cross-Comparison of Vegetation Indices Derived from Landsat-7 Enhanced Thematic Mapper Plus (ETM+) and Landsat-8 Operational Land Imager (OLI) sensors. Remote Sens., 6, 310–329, 2013.

[15] Ke Y., Im J., Lee J., Gong H., Ryu Y. Characteristics of Landsat 8 OLI-derived NDVI by comparison with multiple satellite sensors and in-situ observations. Remote Sens. Environ., 164, 298–313, 2015.

[16] USGS, 2013, http://landsat.usgs.gov/Landsat8 UsingProduct.php

[17] Li Z.L., Tang B.H., Wu H., Ren H., Yan G., Wan Z., Trigo I.F., Sobrino J.A. Satellite-derived land surface temperature: Current status and perspectives. Remote Sens. Environ. 131, 14–37. 2013.